Analysis of 0.8-GeV polarized-proton elastic scattering from ^{208}Pb, ^{90}Zr, ^{58}Ni, and ^{12}C

L. Ray
Los Alamos Scientific Laboratory, Los Alamos, New Mexico 87545

G. W. Hoffmann
University of Texas, Austin, Texas 78712
and Los Alamos Scientific Laboratory, Los Alamos, New Mexico 87545

G. S. Blanpied,* W. R. Coker, and R. P. Liljestrand†
University of Texas, Austin, Texas 78712

(Received 24 February 1978; revised manuscript received 19 June 1978)

Differential cross section and analyzing power data for elastic scattering of 0.8-GeV polarized protons from ^{12}C, ^{58}Ni, ^{90}Zr, and ^{208}Pb have been analyzed in terms of the Kerman-McManus-Thaler formalism using spin-dependent nucleon-nucleon scattering amplitudes. The derived results for nuclear matter densities are in good agreement with theoretical predictions. Uncertainties in the deduced neutron distributions are discussed.

[NUCLEAR REACTIONS ^{12}C, ^{58}Ni, ^{90}Zr, and ^{208}Pb (p,p), $E=0.8$ GeV; cross section and analyzing power; Kerman, McManus, and Thaler spin-dependent optical potential analysis; deduced neutron densities and rms radii; errors in radii given.]

A major goal to be achieved through the analysis of intermediate-energy proton-nucleus elastic scattering data is the determination of the size and shape of the neutron matter density distribution of the target nucleus. This empirical density can be compared with predictions of various self-consistent theoretical models of finite nuclei.[1,2] As discussed previously,[3] the data can be analyzed with the formalism of Kerman, McManus, and Thaler,[4] where the small higher-order terms in the optical potential are neglected.[5,6] Since uncertainties in the nucleon-nucleon scattering amplitudes will be reflected in the deduced neutron densities, improved estimates of the neutron distributions can be obtained by fitting the elastic scattering angular distributions *and* the analyzing powers simultaneously, for a wide range of target nuclei.

This paper presents details of a simultaneous analysis of the angular distribution and analyzing power data obtained at LAMPF for 0.8-GeV proton scattering on ^{12}C, ^{58}Ni, ^{90}Zr, and ^{208}Pb.[3,7] Figures 1 and 2, taken from Ref. 7, display the angular distribution and analyzing power data and theoretical predictions discussed in detail below. The analysis presented here extends the preliminary work discussed earlier in Ref. 3 in that the final, complete analyzing power data have been fitted simultaneously with the angular distribution data and that information obtained from new nucleon-nucleon polarization data at 0.8 GeV (Ref. 8) has been incorporated into the analysis. After presenting the results, the remaining uncertainties in the neutron densities and spin-dependent amplitudes are discussed.

The analysis of the data was carried out as in Ref. 3 by introducing three parameters $\overline{\theta}_p$, $\overline{\alpha}_{sp}$, and $\overline{B}_{sp}$ which are isospin-averages, over the specific target nucleus, of the six nucleon-nucleon spin-dependent parameters. Preliminary proton-proton polarization data at 800 MeV (Ref. 8) indicates that $B_{s,pp} \simeq 0.2\ \mathrm{fm}^2$ so that in the analysis of ^{58}Ni, ^{90}Zr, and ^{208}Pb data $\overline{B}_{sp}$ was fixed to this value. The parameters $\overline{\theta}_p$ and $\overline{\alpha}_{sp}$ were freely searched in order to optimize the fits to the proton-nucleus analyzing power data. For ^{12}C the resulting analyzing power fits were inferior to the other cases, and the effect of varying $\overline{B}_{sp}$ was also investigated. Presumably this additional flexibility partially simulates effects due to the large deformation of ^{12}C, which the simple spherically symmetric potential model does not include.

A general form for the point proton and neutron density distributions was chosen as

$$\begin{aligned}\rho_j(r) = \rho_{0j}\big((1+w_j r^2/R_j^2)/\{1+\exp[(r^k-R_j^k)/z_j^k]\}\\ + s_j\cos(m_j r-\phi_j)\exp[-d_j(r-r_{0j})^2]\\ + s_j\exp[-d_j'(r-r_{0j}')^2]\big)\end{aligned} \tag{1}$$

for $j=p$ or n. The second and third terms in Eq. (1) are used for ^{208}Pb in order to fit the electron scattering data[9] extending beyond $q^2=0.3(\mathrm{GeV}/c)^2$. The additional Gaussian term is required for ^{12}C in order to reproduce electron scattering data while the second (oscillatory) term has been added to the ^{12}C neutron density in order to achieve a

TABLE I. The results of the theoretical analysis discussed in the text. The first four columns give the numerical values of the parameters of Eq. (1) in the text. The root-mean-square (rms) radii for the point-nucleon density distributions are listed in the column under $\langle r^2\rangle^{1/2}$. The quantity $\langle r^2\rangle^{1/2}_{CH}$ is the rms radius of the charge form factor taken from electron scattering. The last three columns give the numerical values of the spin-dependent parameters, Eq. (2) of Ref. 3. Uncertainties in these quantities are discussed in the text.

Nucleus		w	R (fm)	z (fm)	k	$\langle r^2\rangle^{1/2}$ (fm)	$\langle r^2\rangle^{1/2}_{CH}$ (fm)	$\bar\theta_p$ (fm^2)	$\bar\alpha_{sp}$	$\bar B_{sp}$ (fm^2)
^{12}C	p	−0.15	2.42	0.45	1	2.319	2.453	17.6	0.29	0.07
	n	−0.15	2.43	0.46	1	2.393	···	17.6	0.29	0.07
^{58}Ni	p	−0.13	4.30	0.47	1	3.688	3.774	11.8	0.50	0.2
	n	−0.02	4.07	0.50	1	3.652	···	11.8	0.50	0.2
^{90}Zr	p	0.32	4.55	2.41	2	4.204	4.280	11.2	0.55	0.2
	n	0.56	4.49	2.45	2	4.289	···	11.2	0.55	0.2
^{208}Pb	p	0.36	6.45	2.65	2	5.443	5.502	9.0	0.63	0.2
	n	0.36	6.19	3.13	2	5.625	···	9.0	0.63	0.2

good fit to the proton elastic scattering data. The interpretation of such terms is discussed later. The point proton matter distributions were obtained numerically from the nuclear charge densities[9-11] determined from electron scattering, and kept fixed throughout the analysis. Corresponding neutron density parameters, as well as the two spin-dependent parameters, $\bar\theta_p$ and $\bar\alpha_{sp}$ ($\bar B_{sp}$ was also varied for ^{12}C) were freely searched to provide simultaneous fits to both the angular distributions and the analyzing powers, and numerical values are given in Table I. These fits to the analyzing powers for ^{58}Ni, ^{90}Zr, and ^{208}Pb are shown as the solid curves in Fig. 2 and as the dash-dot curve for ^{12}C in the same figure.

Unfolding the proton density for ^{208}Pb from the "model-independent" charge density of Frois *et al.*,[9] yields the three parameter Gaussian density given in Table I along with terms [see Eq. (1)] having $s=-0.03$, $m=1.4$ fm^{-1}, $\phi=2.5$ rad, $d=0.52$ fm^{-2}, $r_0=6.3$ fm, $s'=0.13$, $d'=0.21$ fm^{-2} and $r_0'=0$. Freely searching the neutron density yields the fit shown in Fig. 1 and the parameters given in Table I. Adding small terms to the neutron density did not significantly improve the fit. From the analysis, the difference between the neutron and proton rms radii, Δr_{np}, is 0.18 fm (see Table I) which is in fair agreement with results of analyses[12,13] of 1-GeV Saclay data[14] which give 0.25 fm, and is in good agreement with recent Hartree-Fock predictions[1,2,15] which give $\Delta r_{np}=0.20$–0.23 fm, but disagrees notably with some recent Glauber analyses of 1-GeV Leningrad data[15] which obtain $\Delta r_{np}=0.04$–0.06 fm.[15-16] The Leningrad and Saclay data are also in disagreement, by an amount accounting for the discrepancy.

The new 800-MeV ^{90}Zr data are shown in Figs. 1 and 2 along with the result of the calculation, which yields $\Delta r_{np}=0.085$ fm, while the Hartree-Fock[2] result is 0.07–0.12 fm. A recent Glauber analysis of 1-GeV Leningrad data[15] gave $\Delta r_{np}=0.07$ fm.[16]

The analysis of the ^{58}Ni data, as shown in Fig. 1 of Ref. 3 and Fig. 2, yields $\Delta r_{np}=-0.036$ fm, in good

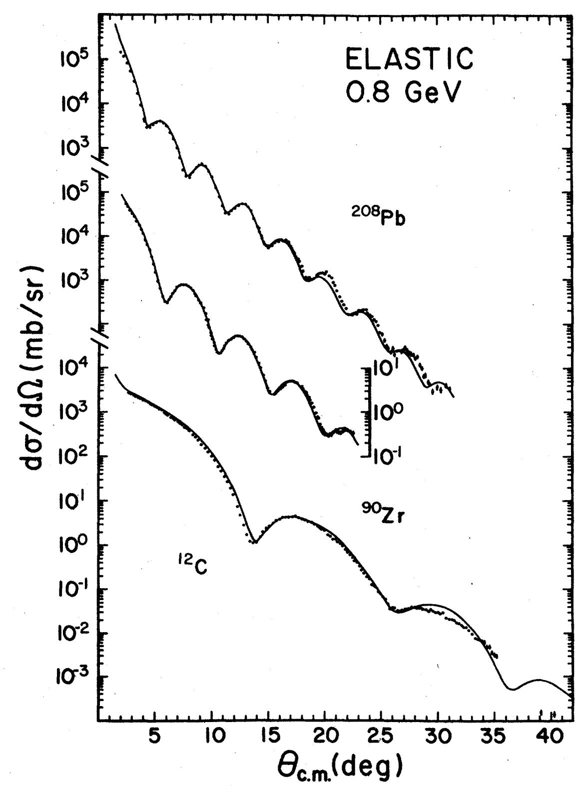

FIG. 1. Elastic angular distributions for 0.8-GeV proton scattering from ^{12}C, ^{90}Zr, and ^{208}Pb and results of theoretical analysis discussed in text.

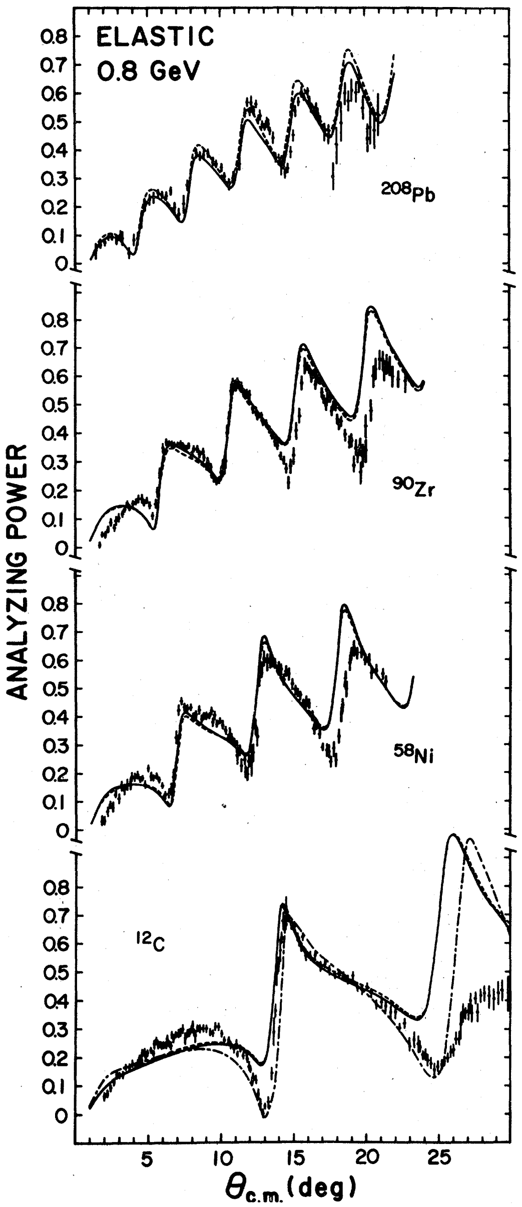

FIG. 2. Elastic analyzing powers for 0.8-GeV polarized proton scattering from ^{12}C, ^{58}Ni, ^{90}Zr, and ^{208}Pb and results of theoretical analysis discussed in text. Dashed curves are obtained from the average spin parameters for ^{58}Ni, ^{90}Zr, and ^{208}Pb (see Ref. 7).

agreement with the Alkhazov *et al.*[17] analysis of 1-GeV data which yields $\Delta r_{np} = -0.043$ fm, with the Chaumeaux *et al.*[18] analysis of the same data which obtains $\Delta r_{np} = -0.07$ fm, and with Hartree-Fock predictions,[19] which give $\Delta r_{np} = 0.00$ fm.

For ^{12}C the spherically symmetric charge density obtained from electron scattering analysis[10] yields, after unfolding, the spherical point proton density given by the three-parameter Fermi form in Table I, plus a Gaussian term with $s' = 0.27$, $d' = 6.9$ fm^{-2}, and $r_0' = 1.4$ fm. Searching $\bar{\theta}_p$ and $\bar{\alpha}_{sp}$ with $\bar{B}_{sp} = 0.2$ fm^2 yields a fit to the analyzing power data given by the solid curve in Fig. 2. Allowing $\bar{B}_{sp}$ to vary yields the improved fit denoted by the dash-dot curve in the same figure. Neither calculation yields fits of the same quality as obtained for ^{58}Ni, ^{90}Zr, or ^{208}Pb. Because of this, considerable ambiguity exists in the choice of spin parameters, which is reflected in a large range of values for $\langle r_n^2 \rangle^{1/2}$ (i.e., $\Delta r_{np} \simeq \pm 0.1$ fm), an effect which is *not* observed for the other three cases studied. For the results shown in Fig. 1, $\bar{B}_{sp}$ was allowed to vary in order to obtain the best fit to the analyzing power data. Setting $\rho_n(r) = \rho_p(r)$ results in a poor fit to the elastic angular distribution, regardless of the spin parameters used, the predicted cross section being low by a factor of from 3 to 5 at 25°–35° c.m. The actual neutron density used in the calculation, which gave the fit to the ^{12}C data as shown in Fig. 1, is a three-parameter Fermi (see Table I) plus an oscillatory term with $s = -0.02$, $m = 2.7$ fm^{-1}, $\phi = 1.7$ rad, $d = 0.33$ fm^{-2}, and $r_0 = 2.6$ fm. The reader is cautioned not to interpret this small term as representing a perturbation to the actual ^{12}C neutron density. Deformation effects, as well as correlations, are unaccounted for in the calculation and spin-dependence is not well reproduced in the high-momentum-transfer region. Rather, this term demonstrates the degree of sensitivity which will be afforded by the data, once all first order and important higher-order terms are properly treated, particularly the large shape deformation peculiar to ^{12}C in this region of momentum-transfer space. Both the present analysis and that of Ahmad[12] are consistent with $\Delta r_{np} = 0$.

Several calculations were carried out to determine the significance of the first-order spin-orbit terms in the determination of the neutron densities of ^{90}Zr and ^{208}Pb. The neutron rms radii deduced with $\bar{\theta}_p = 0$ are generally changed by about 0.03 fm from those found with $\bar{\theta}_p \neq 0$. The density itself, however, is more sensitive, as can be seen in Fig. 3 which shows the neutron densities for ^{90}Zr and ^{208}Pb determined with (solid curve) and without (dash-dot) the spin orbit term. Also shown in Fig. 3 as the dashed curve is the neutron density as found from analysis of the differential cross section data, with the three spin-dependent parameters constrained to the average of the ^{58}Ni, ^{90}Zr, and ^{208}Pb parameters. These densities for ^{90}Zr (^{208}Pb) are identical for $r > 3$ (4) fm to those found by freely searching the spin parameters, and the two densities differ by at most 1.6% for $r < 3$ (4) fm. In all cases, good fits to the angular distributions were obtained. It should be noted that these neu-

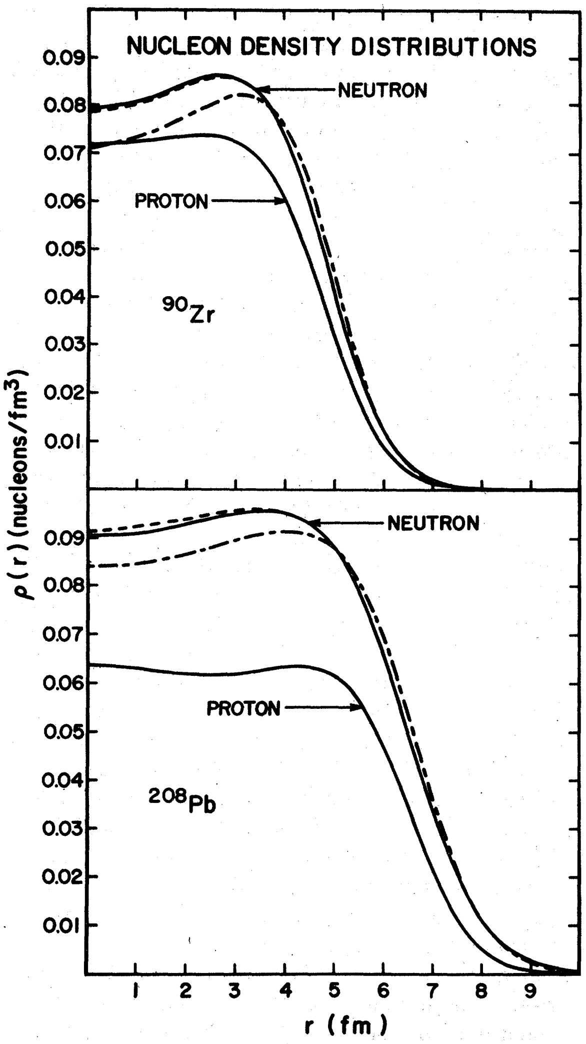

FIG. 3. Upper half: Folded proton and neutron matter densities for ^{90}Zr resulting from analysis including spin-orbit potential (solid curve). The dash-dot curve is the neutron density deduced when the spin-orbit potential is omitted. The density shown by the dashed curve is obtained when the average of the ^{208}Pb, ^{90}Zr and ^{58}Ni spin parameters are used. Lower half: Folded proton and neutron matter densities for ^{208}Pb. Curves have the same meaning as in the upper half.

tron density differences are significant only for $r \gtrsim 3$ (4) fm for ^{90}Zr (^{208}Pb) since the predicted angular distributions are fairly insensitive to the nuclear interior.

An investigation[20] of the effect of systematic sources of error and model dependence on the deduced neutron rms radii, $\langle r_n^2\rangle^{1/2}$, has been made. Systematic errors considered were (1) the overall normalization and determination of scattering angle of the data,[7] (2) beam energy and polarization,[7] (3) proton charge density,[9-11] (4) the two nucleon amplitudes,[21] and (5) the omission in the analysis of Pauli correlations.[5,22]

The procedure adopted to determine the error in the deduced neutron rms radius due to 1–4 above was to individually alter each parameter and recover the original $|\chi|^2$ by variation of the neutron density. The error in $\langle r_n^2\rangle^{1/2}$ due to the omission of target nucleon-nucleon correlations was estimated from the calculated changes in the overall magnitude and slope of the predicted cross sections, as given by Harrington and Varma[22] and by Boridy and Feshbach.[5] The error in the deduced neutron rms radius due to model dependence (resulting from the finite maximum momentum transfer of the data) and the statistical error in the angular distribution data was determined by generating error envelopes[23] using approximately model-independent neutron densities and a technique analogous to that used by Sick[24] in electron scattering analyses. Details of the approach used here will be reported elsewhere.[20] The results of these investigations, for the case of ^{90}Zr, are presented in Table II. The first twelve contributions to the error in the deduced $\langle r_n^2\rangle^{1/2}$ listed in Table II are all approximately independent, and hence add incoherently. The error in $\langle r_n^2\rangle^{1/2}$ due to the omission of the Pauli correlations is not independent of the other errors, and is added linearly to obtain a total uncertainty in $\langle r_n^2\rangle^{1/2}$ for ^{90}Zr of ±0.07 fm. For ^{58}Ni and ^{208}Pb the resulting absolute error in the deduced neutron rms radius is also ±0.07 fm, while for ^{12}C it is ±0.1 fm.

In conclusion, results of an analysis of 800-MeV proton elastic differential cross section and analyzing power data for target nuclei ^{12}C, ^{58}Ni, ^{90}Zr,

TABLE II. Contributions to the error in the deduced neutron rms radius, $\langle r_n^2\rangle^{1/2}$, for ^{90}Zr.

Source[a]	Magnitude	Contribution (fm)
Normalization	±10%	±0.017
$\Delta\theta_{cm}$	±0.03°	±0.021
$\Delta\rho_p(r)$	±0.02 fm	±0.018
ΔT_{lab}	±2 MeV	±0.019
$\Delta\sigma_{pp}$	±0.5 mb	±0.005
$\Delta\sigma_{pn}$	±0.22 mb	±0.002
ΔB_{pp}	±0.005 fm^2	±0.005
ΔB_{pn}	±0.022 fm^2	±0.020
$\Delta\alpha_{pp}$	±10%	±0.001
$\Delta\alpha_{pn}$	±10%	±0.002
$\Delta(\bar{\theta}_p, \bar{\alpha}_{sp}, \bar{B}_{sp})$		±0.022
Statistical and model dependence		±0.015
Pauli correlations		±0.021
TOTAL		±0.072

[a]See Ref. 3 for the nucleon-nucleon parametrization and numerical values used.

and ^{208}Pb have been presented. Realistic errors in the deduced neutron rms radii have been determined. It has been shown that the difference in densities obtained from spin-dependent vs spin-independent analyses (e.g., Fig. 3) is significant near the nuclear surface and that simultaneous analysis of elastic differential cross section *and* analyzing power data removes a systematic error of ±0.03 fm from the deduced neutron rms radii. Finally, the results for Δr_{np}, the neutron-proton rms radius differences, are found to be consistent with recent Hartree-Fock predictions.

This research was supported in part by the U. S. Department of Energy and the Robert A. Welch Foundation.

---

*Present address: New Mexico State University, Las Cruces, New Mexico 88001.

†Present address: TRIUMF, University of British Columbia, Vancouver, British Columbia.

[1]J. W. Negele, Phys. Rev. C 9, 1054 (1974), and references therein.

[2]J. W. Negele and D. Vautherin, Phys. Rev. C 5, 1472 (1972).

[3]G. S. Blanpied *et al.*, Phys. Rev. Lett. 39, 1447 (1977).

[4]A. K. Kerman, H. McManus, and R. M. Thaler, Ann. Phys. (N.Y.) 8, 551 (1959).

[5]E. Boridy and H. Feshbach, Ann. Phys. (N.Y.) 109, 468 (1977).

[6]H. Feshbach, A. Gal, and J. Hüfner, Ann. Phys. (N.Y.) 66, 20 (1971).

[7]G. W. Hoffmann *et al.*, Phys. Rev. Lett. 40, 1256 (1978).

[8]P. R. Bevington *et al.*, Phys. Rev. Lett. 41, 384 (1978).

[9]B. Frois *et al.*, Phys. Rev. Lett. 38, 152 (1977).

[10]I. Sick and J. S. McCarthy, Nucl. Phys. A150, 631 (1970).

[11]C. W. de Jager, H. de Vries, and C. de Vries, At. Data Nucl. Data Tables 14, 479 (1974).

[12]I. Ahmad, Nucl. Phys. A247, 418 (1975).

[13]L. Ray, Ph.D. Thesis, University of Texas at Austin, 1977 (unpublished).

[14]R. Bertini *et al.*, Phys. Lett. 45B, 119 (1973).

[15]G. D. Alkhazov *et al.*, reports (unpublished).

[16]G. K. Varma and L. Zamick, Phys. Rev. C 16, 308 (1977).

[17]G. D. Alkhazov *et al.*, Phys. Lett. 67B, 402 (1977).

[18]A. Chaumeaux, V. Layly, and R. Schaeffer, Phys. Lett. 72B, 33 (1977).

[19]We used the density-matrix-expansion code of J. Negele [see Ref. (2)].

[20]L. Ray, W. R. Coker, and G. W. Hoffmann, to be published.

[21]J. Bystricky, F. Lehar, and Z. Janout, Report No. CEA-N-1547 (E)-Saclay, 1972 (unpublished).

[22]D. R. Harrington and G. K. Varma, report (unpublished).

[23]I. Brissaud and M. K. Brussel, Phys. Rev. C 15, 452 (1977).

[24]I. Sick, Nucl. Phys. A218, 509 (1974).